General Disclaimer

One or more of the Following Statements may affect this Document

- This document has been reproduced from the best copy furnished by the organizational source. It is being released in the interest of making available as much information as possible.

- This document may contain data, which exceeds the sheet parameters. It was furnished in this condition by the organizational source and is the best copy available.

- This document may contain tone-on-tone or color graphs, charts and/or pictures, which have been reproduced in black and white.

- This document is paginated as submitted by the original source.

- Portions of this document are not fully legible due to the historical nature of some of the material. However, it is the best reproduction available from the original submission.

X-621-71-273
PREPRINT

THE ELECTRON HEATING RATE AND ION CHEMISTRY IN THE THERMOSPHERE ABOVE WALLOPS ISLAND DURING THE SOLAR ECLIPSE OF MARCH 7, 1970

L. H. BRACE
H. G. MAYR
M. W. PHARO, III
L. R. SCOTT
N. W. SPENCER
G. R. CARIGNAN

MAY 1971

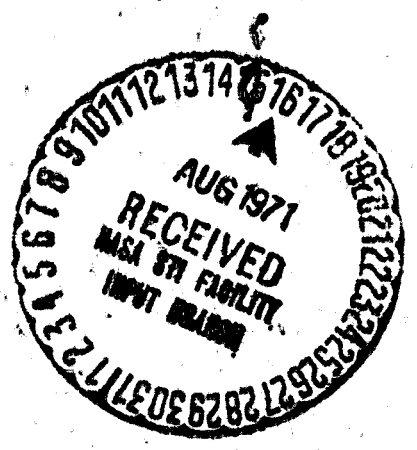

GSFC
GODDARD SPACE FLIGHT CENTER
GREENBELT, MARYLAND

X-621-271-273

THE ELECTRON HEATING RATE AND ION CHEMISTRY IN THE THERMOSPHERE ABOVE WALLOPS ISLAND DURING THE SOLAR ECLIPSE OF MARCH 7, 1970

by

L. H. Brace, H. G. Mayr, M. W. Pharo, III,
L. R. Scott, N. W. Spencer
Goddard Space Flight Center
Greenbelt, Maryland

and

G. R. Carignan
Department of Electrical Engineering
University of Michigan
Ann Arbor, Michigan

May 1971

GODDARD SPACE FLIGHT CENTER
Greenbelt, Maryland

THE ELECTRON HEATING RATE AND ION CHEMISTRY IN THE THERMOSPHERE ABOVE WALLOPS ISLAND DURING THE SOLAR ECLIPSE OF MARCH 7, 1970

L. H. Brace, H. G. Mayr, M. W. Pharo, III,
L. R. Scott, N. W. Spencer
Goddard Space Flight Center
Greenbelt, Maryland

and

G. R. Carignan
Department of Electrical Engineering
University of Michigan
Ann Arbor, Michigan

ABSTRACT

An identical pair of thermosphere probes measured the N_2 concentration and temperature, the ion composition and concentrations and the electron temperature up to 290 kilometers about 30 minutes and 5 minutes before totality during the March 7, 1970 eclipse at Wallops Island. The rockets travelled similar trajectories thus permitting the purelv temporal changes between flights to be resolved. The neutral temperature and N_2 concentration changed little but the electron temperature decreased by as much as 20% in the lower F-region. The ion concentration decreased by about 30% in the F-region and about 50% in the E-region, with little change in relative ion composition. The electron cooling rates decreased by a factor

of 6 in the lower F-region, approximately in proportion to the change in visible solar disc. A smaller than expected decrease in the cooling rate below 150 kilometers between the two flights indicates a hardening of the solar spectrum and suggests a significant heat contribution from the solar corona near totality. The ion composition measurements were consistent with solutions of the ion continuity equations. A proper fit required a factor of three enhancement of the flux below 200 Å, an amount also consistent with the electron heat balance analysis. Reactions involving the minor ions N^+ and N_2^+ were found to be important for the ion chemistry of the major ions O_2^+ and NO^+, especially at the time of eclipse. The negligible response of the neutral atmosphere to the eclipse is reasonable considering the long time constants for the conductive and convective transport processes and the local nature of the disturbance.

INTRODUCTION

The occurrence of a solar eclipse at Wallops Island on March 7, 1970 presented a unique opportunity to investigate the response of the thermosphere and ionosphere to rapidly changing solar illumination at a low zenith angle. The response times of this region depend inherently upon the ion reaction rates, the electron, ion and neutral cooling rates, and perhaps on dynamic effects associated with the rapid changes occurring during the eclipse. To investigate these changes, two identical Thermosphere Probes, NASA 18.104 and 18.105, were launched southeastward from Wallops Island into the path of the approaching cone of totality. At the apogee altitude of 290 kilometers, the percent obscuration had reached 42% and 84%, respectively. The two rockets were launched along essentially identical paths to permit the purely temporal, eclipse-induced changes to be separated from any spatial variations that might otherwise have been encountered.

In this paper, the resulting measurements of ion composition, total ion concentration, N_i, molecular nitrogen concentration $n(N_2)$ and temperature, T_{N_2}, the electron temperature, T_e, are presented and these data are analyzed in terms of the electron heat balance and ion photochemistry.

THE INSTRUMENTS

The Thermosphere Probe (TP) is an ejectable, vacuum-tight package that can carry several instruments to altitudes of about 290 kilometers when

launched by a Nike-Tomahawk vehicle. The TP has been described by Spencer, et al. (1965, 1969). Briefly, the Thermosphere Probe is a long cylindrical package that is ejected from a clam-shell nose cone at about 70 kilometers, ascends to apogee and returns to the Earth. After ejection, the TP tumbles end over end in a nearly vertical plane with a period of typically three to four seconds, thus exposing its instrument sensors to essentially all angles of attack during each tumble.

The instruments employed in each of these two flights were an omegatron mass spectrometer, a Bennett ion mass spectrometer, and a cylindrical electrostatic probe. These instruments have been described elsewhere (Spencer, et al., 1965, 1969), (Pharo, et al., 1971), (Taylor, et al., 1963, 1965). The omegatrons were tuned to N_2 and measured the height profiles of N_2 over the altitude range between 140 to 290 kilometers. The neutral gas temperatures were derived from the scale height of the N_2 profiles. The ion spectrometer (Pharo and Scott, 1971) measures the ion concentrations in the mass range from 12 to 36 AMU, sweeping at a rate of about 5 times per second.

The cylindrical probe experiment employed two redundant rhodium plated collectors and sweep voltage rates of 22 and 80 volts per sec. A sweep repetition rate of 8 per second was employed. The electron temperatures, T_e, were derived from both probes in the usual manner of fitting an exponential to the retarding region (Brace, et al 1970). The ion concentrations, N_i, were derived from the ion currents collected when the probe was perpendicular to the velocity

vector, following the method described by Taylor, et al. (1963). Details of the data processing for these flights will not be discussed in this paper.

THE MEASUREMENTS

The pre-totality launch times of 1800 UT (1300 EST) for NASA 18.104 and 1827 UT (1327 EST) for NASA 18.105 were selected to permit resolvable changes to occur in the various measured parameters without encountering the non-linear rates of change that might be expected near totality (Stubbe, 1970). This was expected to simplify the theoretical analysis of the measured profiles. The area of unobscured solar disc, as viewed from the rocket trajectories, changed by a factor greater than four between the two flights thus assuring significant changes in solar energy input. As noted earlier, the obscuration at apogee of the two flights was 42% and 84%, respectively. Figure 1 shows the path of totality as it passed Wallops Island at 18:38 UT and the locations of apogee and the 100 kilometer ascent and descent crossings of the two flights. The first rocket reached apogee at 18:04 UT and the second at 18:31 UT. Figure 2 shows the percent obscuration along each leg of the trajectory. The descent data were selected for detailed analysis because of the generally smaller angles of attack for the N_2 and ion measurements and the larger percent obscuration. Figure 3 shows the $n(N_2)$ profiles measured at these times and the corresponding T_{N_2} profiles derived from the N_2 scale heights. The T_e profiles are also shown. There was essentially no resolvable change in either $n(N_2)$ or T_{N_2}

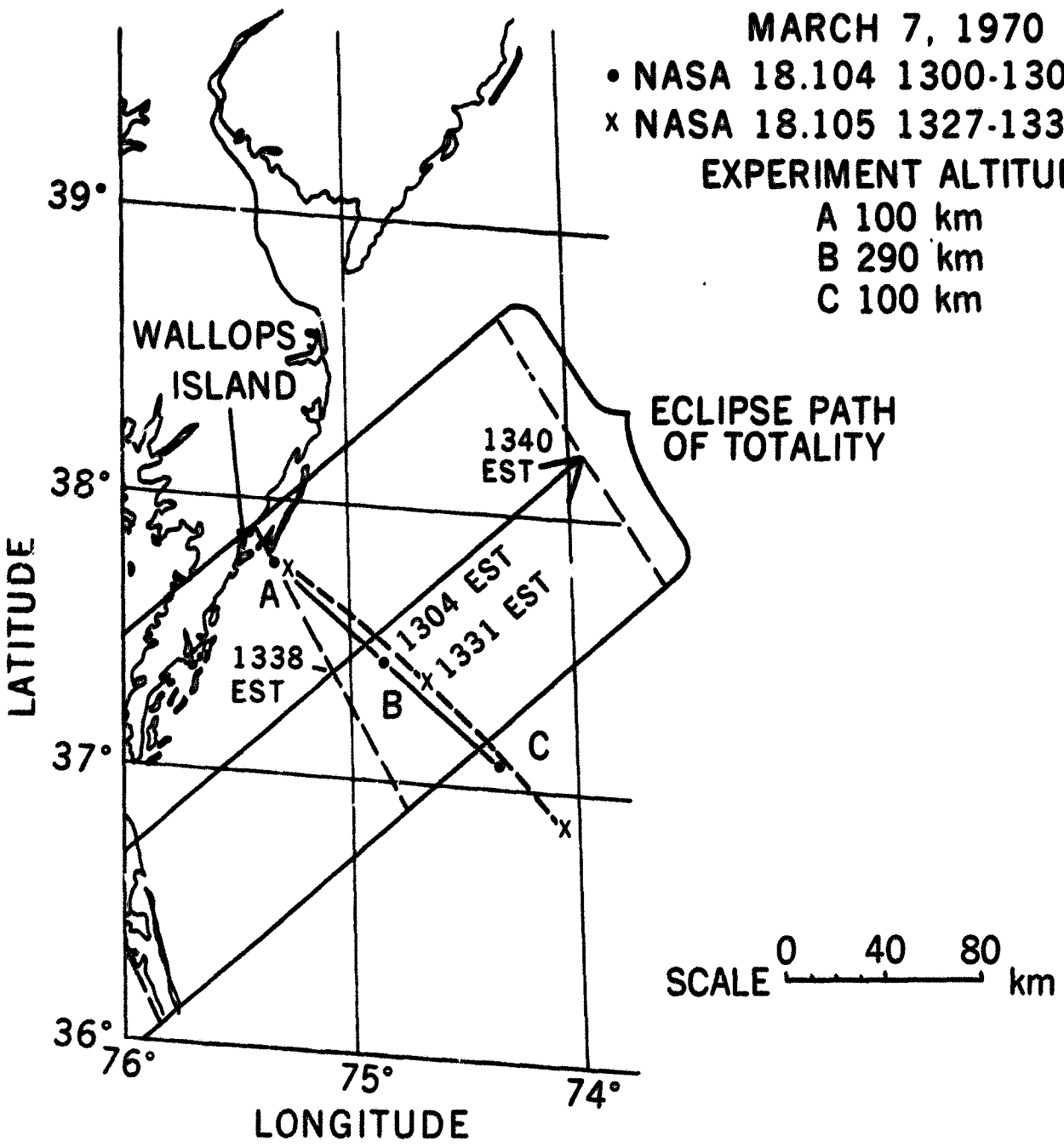

Figure 1. The Trajectories of NASA 18.104 and 18.105 Relative to the Path of the Eclipse. The Instruments Travelled along Approximately the Same Trajectories, Reaching Apogee about 34 Minutes and 7 Minutes before Totality.

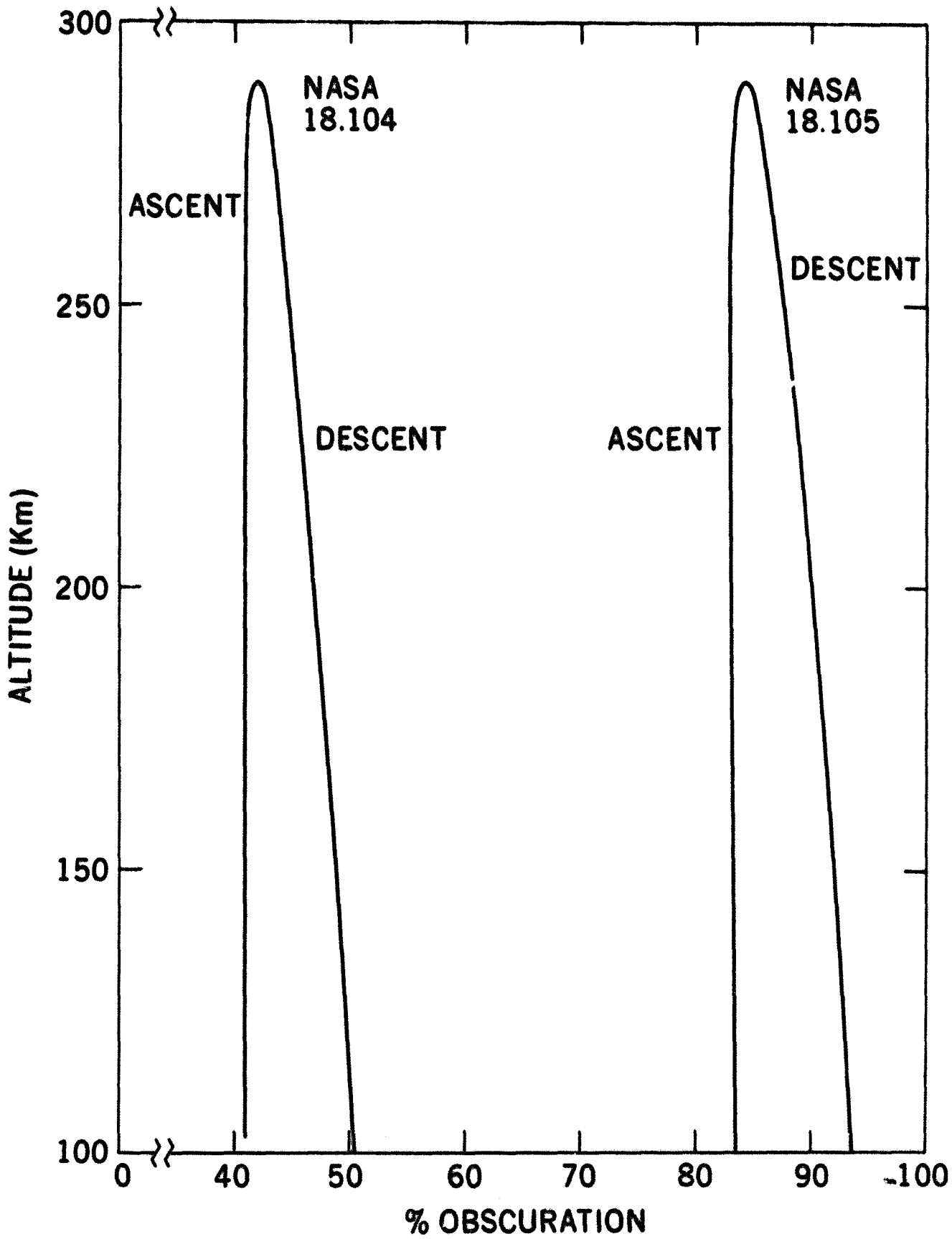

Figure 2. The Percent Obscuration Encountered Along the Trajectories of the Flights. Data from the Descent Leg of Both Flights Have Been Employed in This Paper.

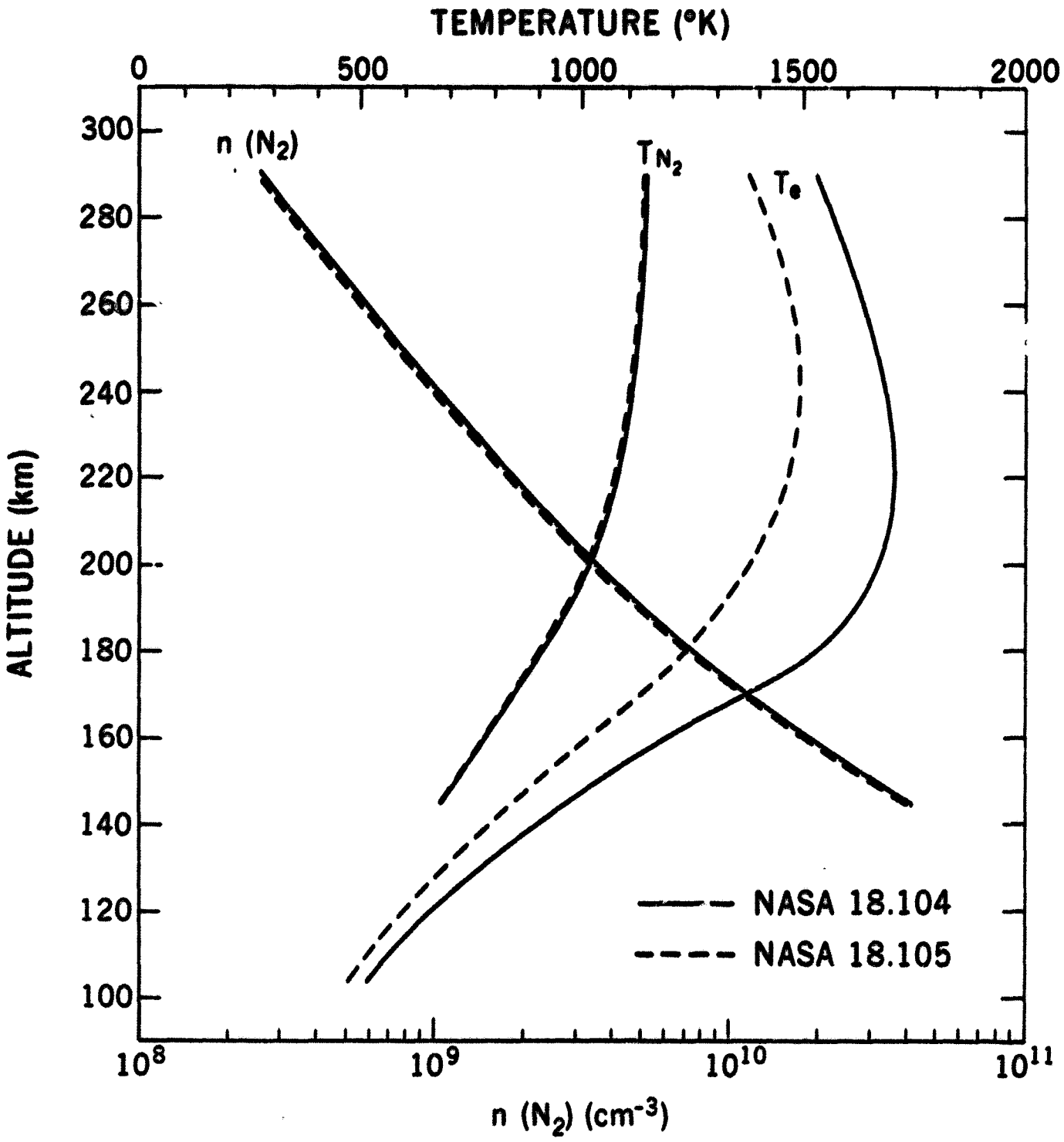

Figure 3. The $n(N_2)$, T_{N_2} and T_e Measurements Taken on Descent of the Two Flights.

within the 5% relative accuracy of these measurements. T_e decreased at all altitudes with the greatest decrease, 20%, occurring at 200 kilometers.

The ion concentration profiles from the two flights, shown in Figure 4, were derived by normalizing the constituent ion currents to the total ion concentration N_i derived from the probe experiment. The latter agreed well with the N_e profiles derived from simultaneous ionosonde records taken at Wallops Station (Jackson and McQuillan, 1970) except in the F_1 region where the N_i values were 10-15% lower. The 5-10% agreement in the E and F_2 regions is considered acceptable considering the horizontal distance between Wallops and the descent legs of the trajectories. Tables I and II are tabulations of the measurements taken on descent of the two flights.

ACCURACY OF THE MEASUREMENTS

The factors that affect the absolute and relative accuracy of these measurements have been treated elsewhere, but it is appropriate to reiterate those factors that are especially important for the eclipse study. Since the goal of this investigation was to resolve the changes in each parameter during the eclipse we have attempted to maintain high relative accuracy by making the two sets of instruments as identical as possible. For this reason the omegatrons were calibrated simultaneously for N_2 on the ground pressure calibration system normally used for this purpose. Their relative accuracy should be better than 5%, including the possible errors in knowledge of the angle

of attack as measured by earth and sun sensors on both flights. The T_{N_2} accuracy is also believed to be better than 5%.

The accuracy of the probe measurements of T_e were estimated to be 5% on the basis of the quality of the exponential fits to the retarding regions and the good agreement between the measurements from the two identical probes on each flight. The N_i values were estimated to be accurate within 10% based on their agreement with the ionosonde N_e profiles in the ascent E-region and F-region essentially above Wallops Island.

The concentrations of the constituent ions are expected to be accurate within 20%. Before they were normalized to the N_i profiles the individual ion currents were corrected for mass discrimination within the spectrometer using the same factors as used in previous applications (Pharo, et al., 1971).

The Neutral Atmosphere Model Adopted

Since the physical interpretation of these data relies in part on a knowledge of the neutral composition of the thermosphere at the times of these flights, we have adopted the Jacchia Model that most closely matches the $n(N_2)$ and T_{N_2} profiles. Figure 5 and Table III represent the model used in the subsequent analyses of these data. To aid in matching the model, we extended the N_2 and T_{N_2} profiles downward by interpolation with the

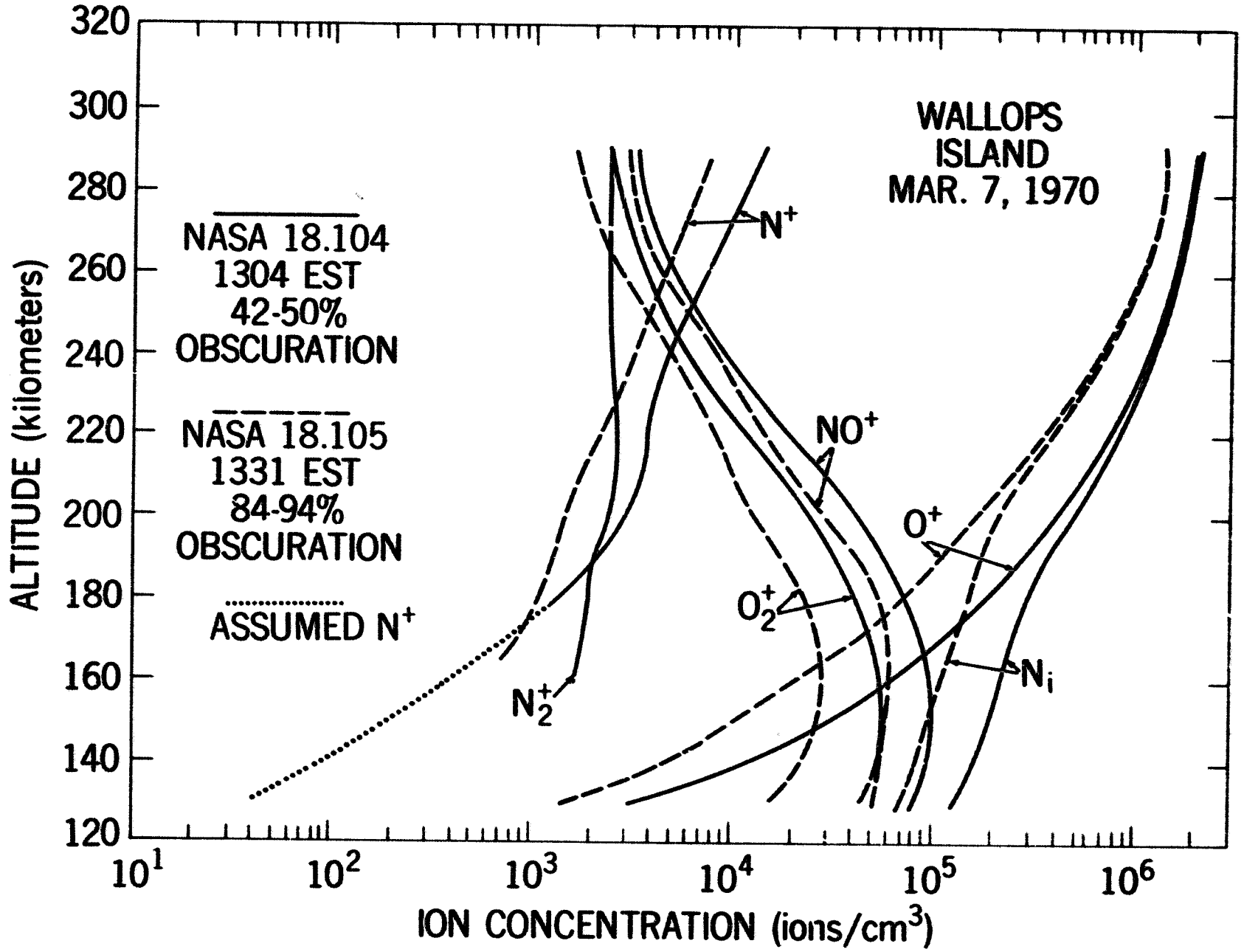

Figure 4. The Ion Composition Profiles.

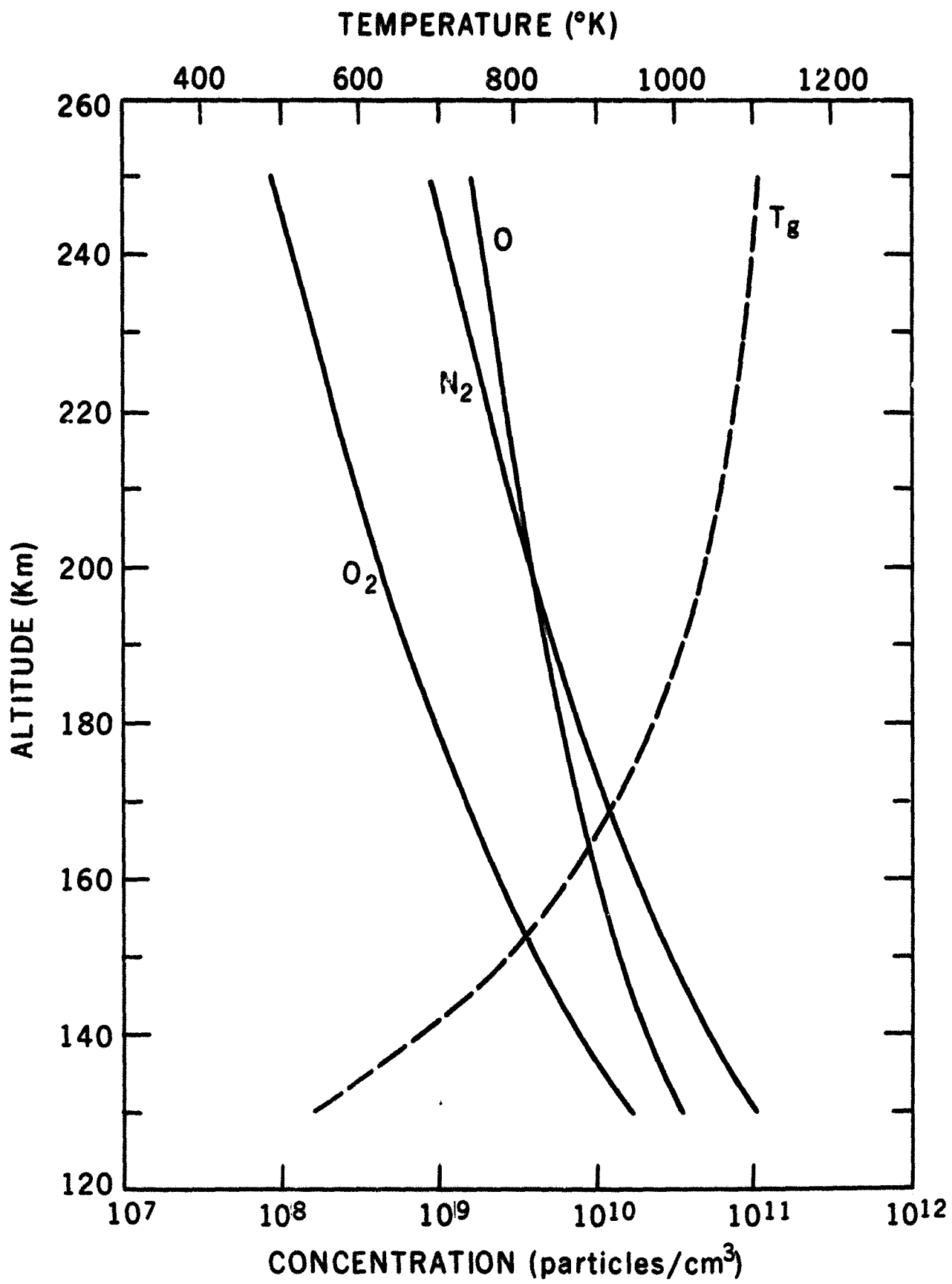

Figure 5. The Jacchia Model Atmosphere Best Matching the $n(N_2)$ and T_{N_2} Profiles Measured on These Flights.

essentially simultaneous Pitot-probe measurements of Horvath and Theon (1971) who measured the total atmospheric density and temperature up to 120 kilometers.

Magnetic Disturbance

It should be noted that the eclipse occurred during a period of large magnetic disturbance. Table IV lists the 3-hour magnetic index, a_p, for a three day period centered on the eclipse day. a_p was 67 at the time of these flights (see box in Table IV). This could be an important factor in the interpretation of the eclipse data, as there is increasing evidence that storms affect the temperature and composition of the neutral atmosphere (Jacchia, et al, 1967) at ionosphere heights thus altering the ion chemistry and thermal balance. We have not attempted to consider the storm effects explicitly, however.

DISCUSSION

The response of the Thermosphere to a solar eclipse is of considerable interest as the solar obscuration introduces abrupt and, to some extent, calculable changes in the energy input to this region. Observations of the thermospheric response to the eclipse in turn provide the opportunity to test our theoretical understanding of the processes controlling its energy and chemical balance. These have been examined in the past using data obtained under normal daytime conditions (Brace, et al, 1969) (Pharo, et al, 1971). In this paper we employ the same type of analysis to eclipse time measurements. In particular we have examined primarily the changes in concentration and temperature observed

between flights to evaluate the changing energy input and photochemical balance during the onset of the eclipse.

The Energy Balance

The magnitude of the electron temperature in the lower ionosphere is primarily determined by the local equilibrium between the electron heating and cooling rates (Hanson, 1962) (Dalgarno, et al., 1963). The electrons are created as photoelectrons that, in their thermalization process, heat the ambient electron population. The latter are cooled by elastic and inelastic collisions with ions and neutrals. Although the heating rate is difficult to calculate lacking simultaneous solar euv information, its equivalent, the cooling rate, can be calculated readily from the measurements of these flights. In this section, we consider the electron heat balance in an attempt to evaluate the effects of the changing solar obscuration during this eclipse.

Following Brace, et al., (1969), the T_e, T_{N_2}, N_i, and $n(N_2)$ profiles, and the selected Jacchia model atmosphere (Figure 5), were employed to calculate the electron cooling rates during these flights. We included the effects of heat conduction (Banks, 1966) and the ion heating induced by thermospheric winds (Stubbe and Chandra, 1970), with a range of wind velocities assumed independent of height. The temporal variation of the internal energy was neglected, as a simple calculation shows that it contributed less than 1% to the energy budget for the small changes that occurred during the eclipse.

Figure 6 shows the resulting cooling rates Q_e (104) and Q_e (105) from the two flights, where the family of curves represents the range of wind velocities assumed. The effects of winds become increasingly important above 220 km where the winds may cause Ti to exceed Tg. The effects of heat conduction represent an additional uncertainty in the cooling rates at high altitudes. The heat conduction flux depends strongly upon the height gradient of T_e, a factor that cannot be derived accurately at the higher altitudes where the horizontal motion of the rocket and temporal changes may be comparable to the altitudinal variation of T_e. However, below 220 kilometers, the wind and heat conduction effects become negligible compared to local cooling, and the validity of the cooling rate profiles depends only upon the accuracy of the measurements and the model.

Figure 6 also compares the ratio of the cooling rates from the two flights (solid) with the ratio of the unobscured solar disc areas (dashed). If the heat sources arose entirely from radiation from the visible disc, these ratios would be comparable, and this appears to be approximately true in the range from 150 to 220 kilometers. However, at lower altitudes, the cooling rates did not decrease proportionally to the decrease in the visible solar disc, suggesting that some of the energy for this region originates outside the visible disc. This is not surprising because solar X-rays originating in the corona are a known source of E-region ionization and heating. Similar evidence for a "residual flux" was reported by Smith, et al., (1965) who found little change in T_e at lower altitudes during the South American eclipse of 1967.

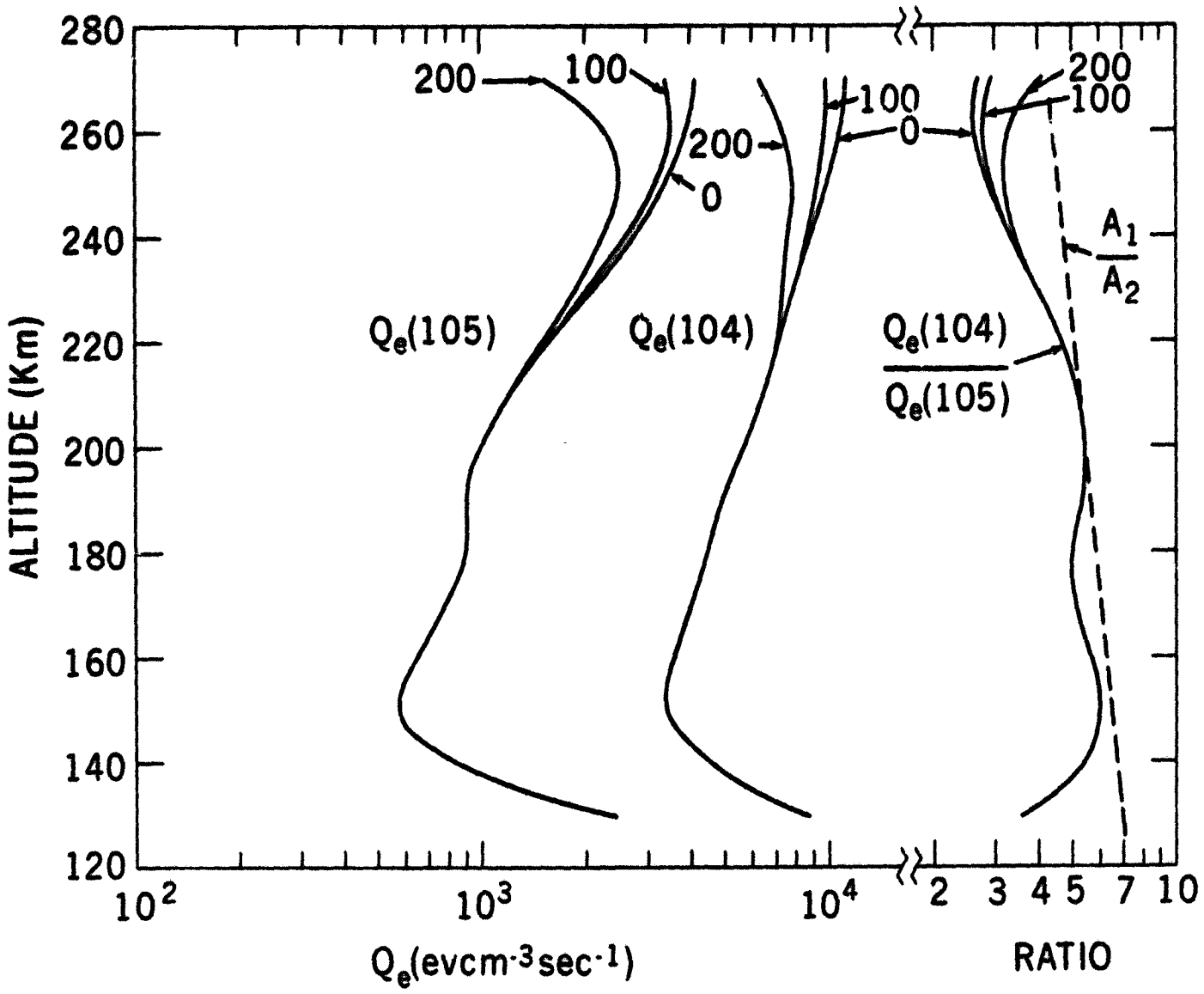

Figure 6. The Cooling Rates Calculated from NASA 18.104 and 18.105 Profiles and Their Ratio Q_e (104)/Q_e (105). Wind Heating of the Ions Is Included for Speeds of 0, 100, 200 Meters/Sec. The Ratio of Unobscured Solar Areas A_1/A_2 Is Shown for Comparison.

The Ion Chemistry

In our analysis of the ion chemistry, we adopted the ultraviolet spectrum of Hinteregger, et al., (1965) and scaled it upward linearly in accordance with the higher level of solar activity at the time of the eclipse ($F_{10.7} = 171$). We then included the solar obscuration effect at each point along the trajectory and exposed the model atmosphere to these euv fluxes and, following Pharo, et al. (1971), calculated the height profiles of each ion constituent. This approach was modified to consider possible transient effects by including in the continuity equations the changes observed between flights in the various ion constituents. This correction was particularly important for the second flight where it accounted for about 30% of the O^+ concentration above 200 kilometers. For all other ions, the effect was less than 4%. From this it is perhaps valid to generalize that a steady state solution of the continuity equation is appropriate even during an eclipse for all ions except O^+.

The neutral atmosphere model used for the ion chemistry analysis was identical to that used in the cooling rate calculations, and the T_e measurements were employed to calculate the temperature dependent recombination rates.

These initial calculated ion profiles (not shown) were found to agree with the measured ion profiles within a factor of two. This might be considered reasonable agreement in view of the uncertainty in the magnitude of the euv flux, the hardening of the euv spectrum implied by the cooling rate profiles, and the uncertainty in the absorption and ionization rates. The most pronounced

deficiency in the initial theoretical result was the low O^+ concentration below 200 kilometers, a deficiency that in turn affected the other ion concentrations.

To attain a better fit to the measurements, two modifications were made. First, the absorption and ionization rates were increased by a factor of two from the values given by Hinteregger et al. (1965) and used by Pharo et al. (1971) on non-eclipse measurements. These changes are within their quoted uncertainties. Secondly, we decreased the rate coefficient for the reactions

$$O^+ + N_2 \longrightarrow NO^+ + O$$

from

$$6.5 \times 10^{-13} \text{ to } 3 \times 10^{-13} \text{ cm}^3 \text{ sec}^{-1}$$

and

$$O^+ + O_2 \longrightarrow O_2^+ + O$$

from

$$5.9 \times 10^{-12} \text{ to } 3.5 \times 10^{-12} \text{ cm}^3 \text{ sec}^{-1}.$$

Both of these rates are lower than laboratory derived rates (Dunkin et al., 1968) by about a factor of two.

To introduce the amount of hard radiation that was inferred from the smalier than expected change in cooling rates, the euv spectrum was scaled upward by a factor of three below 200 Å, as shown schematically in Figure 7. Since the visible solar disc was only 7% in the E-region of the second flight, this factor of three scaling suggests that 14% of the radiation at these wavelengths

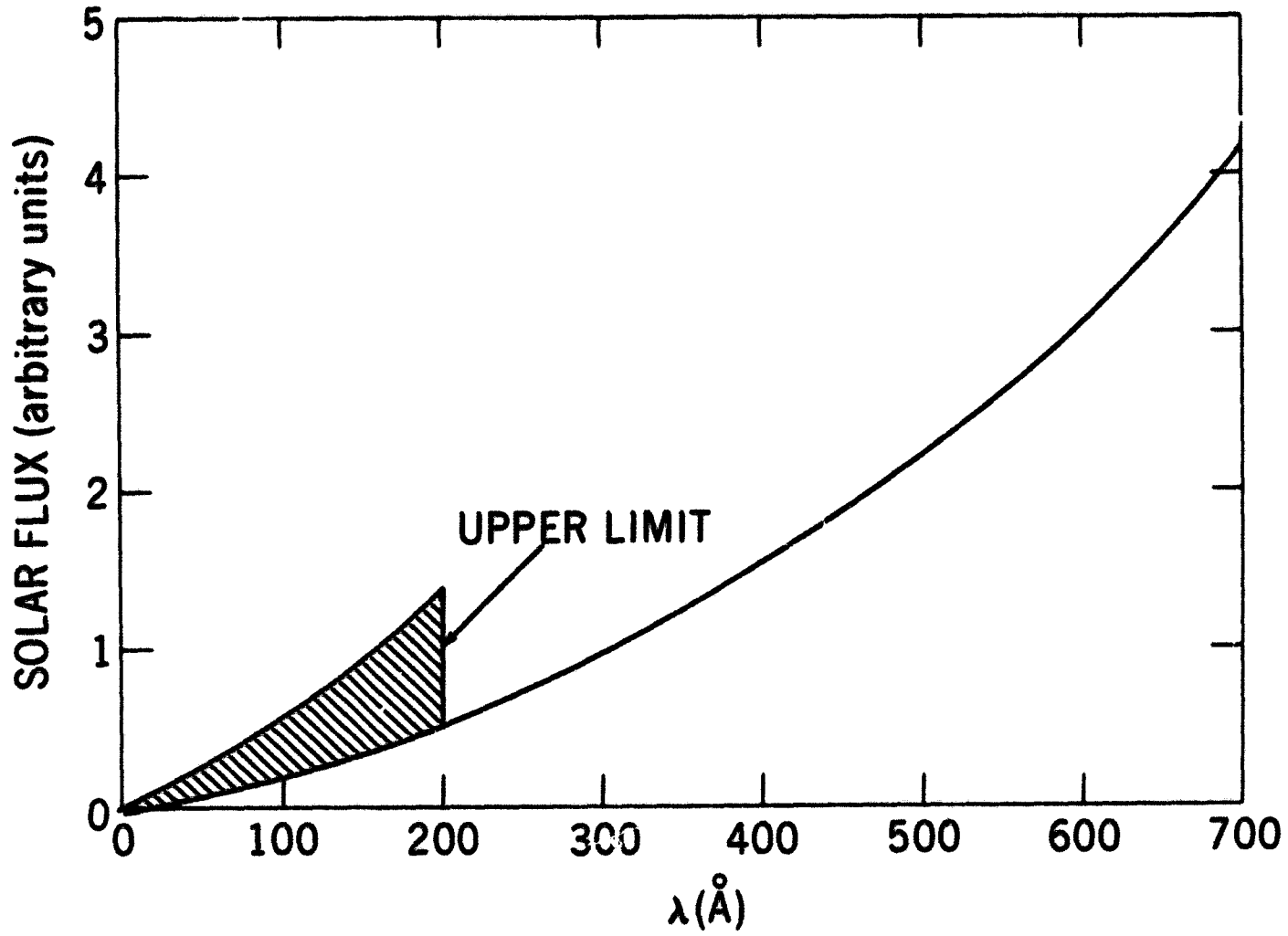

Figure 7. Schematic Model Used for Additional Hard Radiation (Hatched) Needed to Account for the Excess Electron Heating Rates and Deficiency of O^+ on the Second Flight. A Factor of Three Enhancement Was Assumed at Wavelengths Below 200 Å. Detailed Spectrum Is Not Shown.

originated outside the obscured area. From this one would predict that the x-rays are only about 86% obscured by the moon during totality.

The effect upon the O^+ population of intensifying the hard radiation by this scheme is shown in Figure 8. The relative enhancement of $n(O^+)$ is shown for three altitudes assuming the upper wavelengths of 100, 200, 300, 400, and 500 Å, respectively. The wavelengths above 300 Å are relatively less effective at low altitudes. Most of the desired enhancement results from wavelengths between 100 and 200 Å.

The final theoretical ion profiles are shown (dashed) in Figures 9 and 10, and are compared with the measured ion profiles (solid). The agreement is generally better than 15% and thus appears to fall within the combined experimental uncertainties.

Uniqueness of the Analysis

It should be recognized that the analysis that lead to the theoretical ion profiles of Figures 9 and 10 is not entirely unique with respect to the absolute values of ion concentration. Perhaps the greatest uncertainty lies in our ignorance of the solar euv spectrum at the time of the eclipse. Had we used a spectrum different from that presented by Hinteregger et al (1965), somewhat different adjustments of the ionization, absorption, and reaction rates would have been necessary to fit the observations.

However our conclusion that a hardening of the spectrum occurred during the eclipse is on firmer ground as it is based solely on the relative

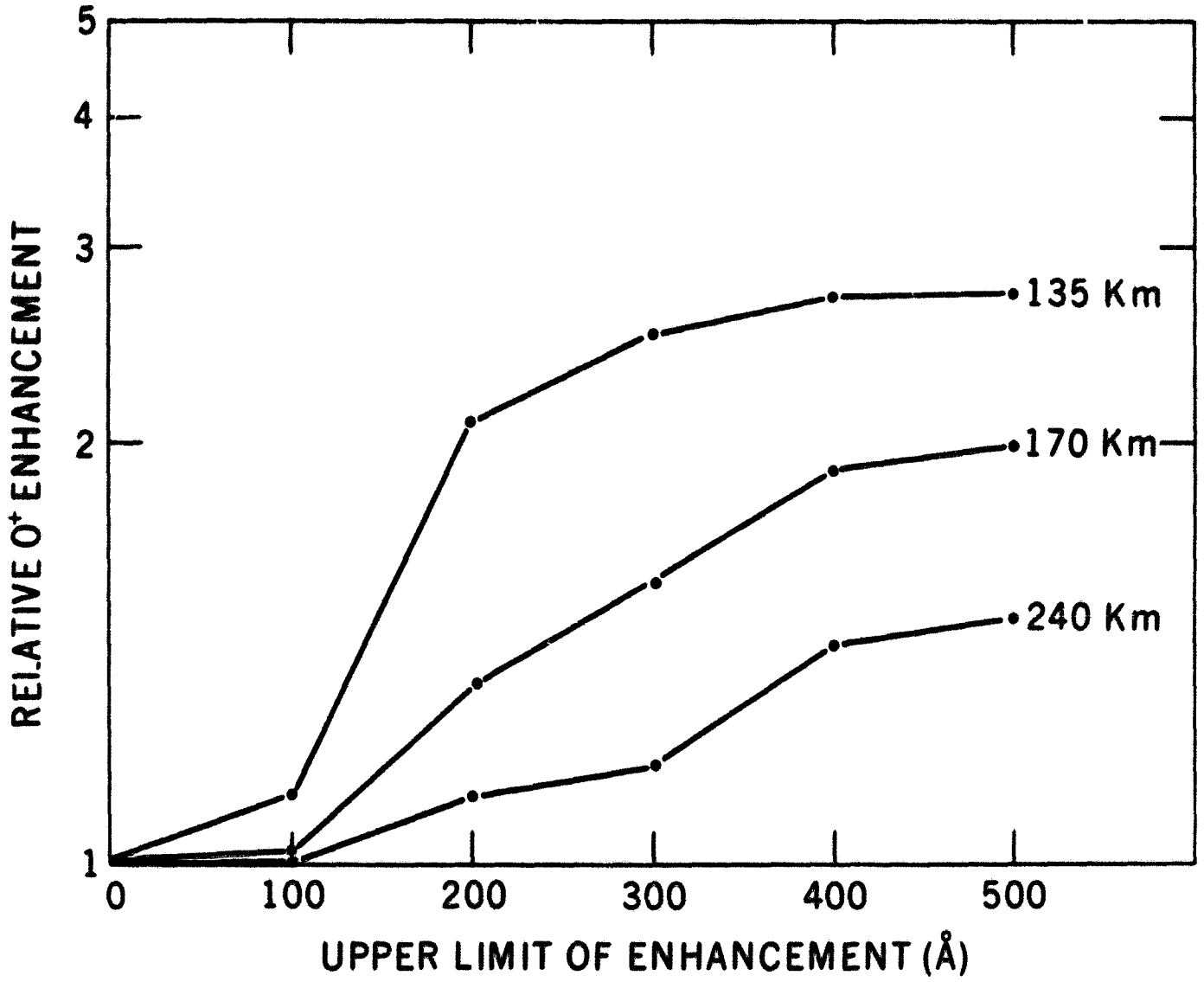

Figure 8. The Relative Enhancement of O^+ at 135, 170 and 240 Kilometer Caused by the X-ray Enhancements of the Type Shown in Figure 7 Assuming Upper Limits of 100, 200, 300, 400 and 500 Å. The Major O^+ Enhancement at Low Altitudes Occurs for Wavelengths Between 100 and 200 Å.

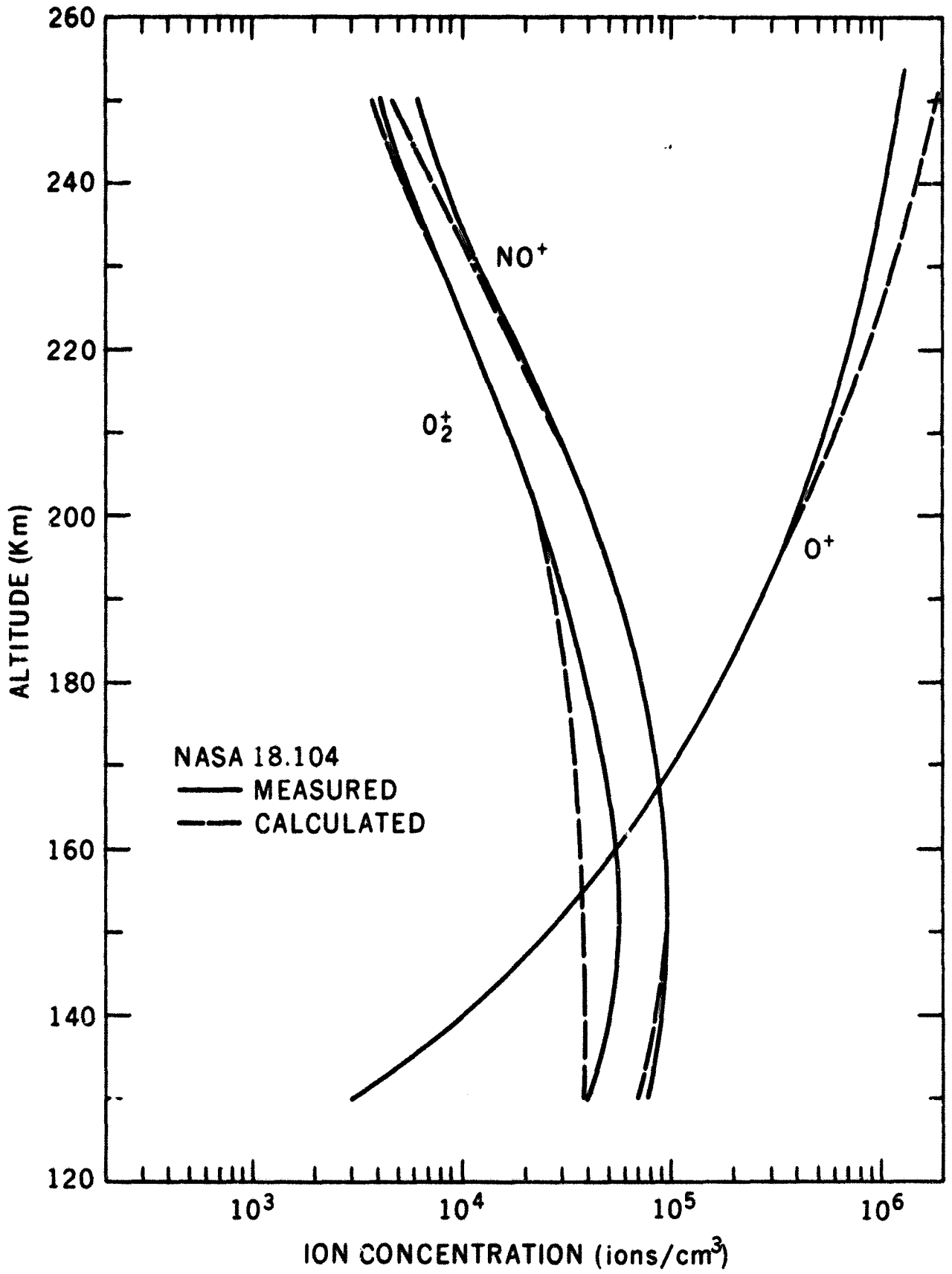

Figure 9. Comparison of 18.104 Ion Measurements (Solid) with Theoretical Profiles (Dashed) Calculated for the Corresponding Solar Obscuration, Including the Enhanced X-ray Component.

changes in the ion concentrations and electron temperatures between the two flights. The changes in these parameters require enhancements in the 100-200 Å range. The form we chose to introduce this enhancement (Figure 7), is not unique, however.

The Effects of the Minor Ion Reactions

The calculations of Stubbe (1970) for this eclipse disagree significantly with regard to the behavior of ion composition during the eclipse. Although some of the discrepancy could be accounted for by suitably modifying the solar euv input, one reason for the failure in Stubbe's model to predict the NO^+ and O_2^+ correctly is because it does not consider the role of the minor constituents N^+ and N_2^+ in the following reactions:

$$N^+ + O_2 \longrightarrow NO^+ + O$$
$$N^+ + O_2 \longrightarrow O_2^+ + N$$
$$N_2^+ + O_2 \longrightarrow O_2^+ + N_2$$
$$N_2^+ + O \longrightarrow NO^+ + N$$

Both of the N^+ reactions are important as the N^+ concentrations are significant in the lower ionosphere and their rates are of the order of 5×10^{-10} cm^3 sec^{-1} (Fehsenfeld, et al., 1965) (Ferguson, 1967). To illustrate the importance of N^+, we have included in Figure 10 the solutions in which these reactions have been neglected (dotted). Without N^+, the O_2^+ concentrations are a factor of 3 too low at 160 km and NO^+ is low by almost a factor of 2. The N_2^+ reactions have less influence on the O_2^+ and NO^+ concentrations but are not negligible. They account for about 20% of the O_2^+ and NO^+. Pharo, et. al., (1971) have

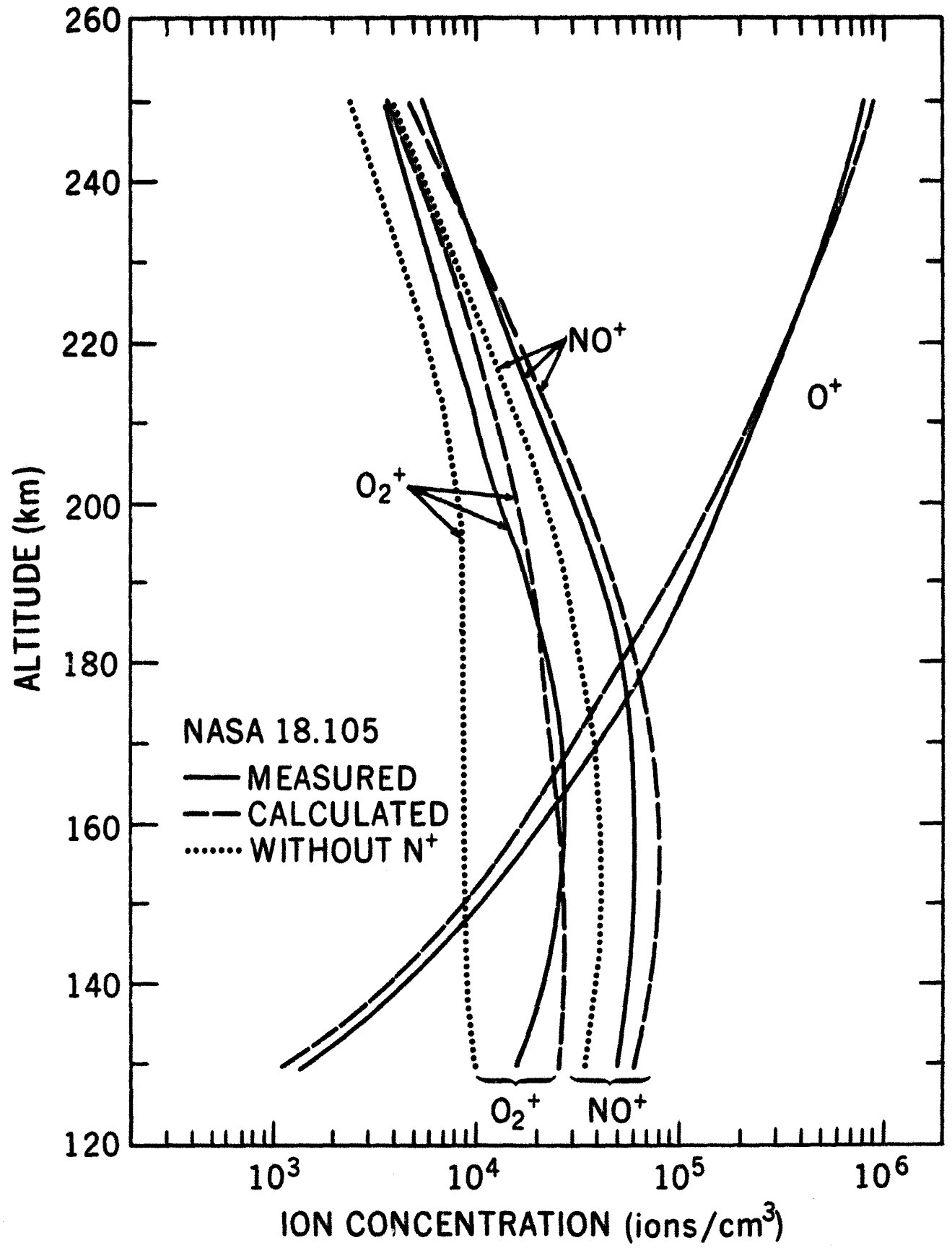

Figure 10. Comparison of 18.105 Ion Measurements with Theoretical Profiles, with X-rays Included. The Dotted Lines Represent the O_2^+ and NO^+ Calculations with the N^+ Reactions Omitted.

included these reactions in their analysis of the normal daytime thermosphere above Wallops Island and obtained similarly good fits to the composition measurements.

The Neutral Atmosphere

It is perhaps appropriate to comment upon the apparent lack of response of the neutral atmosphere to the eclipse. As noted earlier, no resolvable changes in $n(N_2)$ or T_{N_2} occurred between these flights. However, owing to the magnetic disturbances occurring at the time of the eclipse ($a_p = 67$) and throughout at least the previous 24 hours, one should perhaps not assume that the response to the eclipse was entirely normal. Any energy transport from higher latitudes would tend to mask the eclipse effect and further contribute to a smaller response of the atmosphere.

For two other reasons it remains understandable that the eclipse caused little change in the neutral atmosphere. The first is related to the long response time of the neutral atmosphere and the second is related to the highly localized nature of the eclipse.

The total internal energy in a 1 cm^2 column above 120 km is about

$$Q \approx 5 \times 10^4 \text{ ergs cm}^{-2}.$$

This energy can be conducted downward at the 120 km level with a flux of 2.7×10^{-1} ergs cm^{-2} sec^{-1} with a resulting characteristic time of about 1.85×10^5 sec or about 51 hours, a time much greater than the 27 minutes between the flights. Furthermore, vertical and horizontal heat convection (Volland and

Mayr, 1970) can supply energy to and from the adjacent atmosphere at rates of 5×10^{-1} erg cm^{-2} sec^{-1} and 4×10^{-1} erg cm^{-2} sec^{-1}, respectively, leading to characteristic times of the order of 1×10^{5} sec. These also are much longer than the eclipse time, thus it is not surprising to find little change during the eclipse. Since the solar obscuration affects only a very small region at any given instant, horizontal transport tends to fill up this "energy hole" from the adjacent and fully illuminated regions without significantly affecting the global energy budget. The effect of this process is to further damp the eclipse response of the thermosphere. This aspect has been considered by Volland and Mayr (1971) who show that small scale energy disturbances are ineffective in exciting density variations. The excitation efficiency varies as $1/n^2$, where n is the wavenumber corresponding approximately to the ratio of the global dimension to the size of the disturbance.

Stubbe (1970) predicted that the exospheric temperature would decrease during the eclipse, at the end of the eclipse falling about 120° lower than its normal day value. However, Stubbe's model overestimates the variations to be expected during the eclipse. It is one dimensional and therefore does not consider the damping effects of horizontal mass and energy transport, factors that are expected to be significant.

CONCLUSIONS

Measurements of ion, electron and neutral particles at two times during the eclipse have permitted the electron heat balance, the ion chemistry and the neutral atmospheric response to be evaluated. Both the electron heat balance and ion chemistry suggest a hardening of the solar spectrum as the eclipse progresses, with X-rays attenuated about a factor of three less than the euv flux. The euv flux appears to have been attenuated in proportion to the visual obscuration. The role of the minor ions N^+ and N_2^+ is found to be important in the production of NO^+ and O_2^+. These minor ions are usually neglected, but are especially important during an eclipse when photoionization sources for NO^+ and O_2^+ are less significant. The lack of variation of neutral temperature and concentration appears consistent with the long thermal and transport time constants of the thermosphere.

REFERENCES

1. Banks, P. M. "Collision frequencies and energy transfer of ions" Planet. Space Sci., 14, 1105 (1966).

2. Brace, L. H., J. A. Findlay, and G. R. Carignan "Experimental evaluation of ionosphere electron temperature measurements by cylindrical electrostatic probes" Space Res. XI, North-Holland Publishing Co., Amsterdam (1970).

3. Brace, L. H., H. G. Mayr and G. R. Carignan "Measurements of electron cooling rates in the midlatitude and auroral zone thermosphere" J. Geophys. Res., 74, 257, (1969).

4. Dalgarno, A., M. B. McElroy, R. J. Moffett, "Electron temperature in the ionosphere" Planet. Space Sci., 11, 463, (1963).

5. Dunkin, D. B., F. C. Fehsenfeld, A. L. Schmeltekopf, and E. E. Ferguson "Ion-Molecule reaction studies from 300 to 600°K in a temperature controlled flowing afterglow system" J. Chem. Phys., 49, 1365, (1968).

6. Fehsenfeld, F. C., A. L. Schmeltekopf, E. E. Ferguson, "Correction in the laboratory measurement of the rate constant for $N_2^+ + O_2 \rightarrow N_2 + O_2^+$ at 300°K" Planet. Space Sci., 13, 919, (1965).

7. Ferguson, E. E., "Ionospheric ion-molecule reaction rates", Rev. Geophysics, 5, 305, (1967).

8. Hanson, W. B., "Electron temperature in the upper atmosphere" Space Res. III, North-Holland Pub. Co., 282, (1962).

9. Hinteregger, H. E., L. A. Hall, G. Schmidtke, "Solar XUV radiation and neutral particle distribution in July 1963 thermosphere" Space Res. V, North-Holland Publishing Co., 1175, (1965).

10. Horvath, J. J., J. S. Theon, "Response of the neutral particle upper atmosphere to the solar eclipse of 7 March 1970" GSFC document X-May (1971).

11. Jacchia, L. G., J. Slowey, F. Verniani, "Geomagnetic perturbations and upper atmosphere heating" J. Geophys. Res., 72, 1423, (1967).

12. Jackson, J. E., and C. J. McQuillan "The behavior of the ionosphere above Wallops Island during the eclipse of 7 March 1970" GSFC document X-625-70-394, Oct. (1970).

13. Pharo, M. W., III, L. R. Scott, H. G. Mayr, L. H. Brace, and H. A. Taylor, "An experimental study of the ion chemistry and thermal balance in the E and F regions above Wallops Island" Planet. Space Sci., 19, 15, (1971).

14. Pharo, M. W., L. R. Scott, "Observations of thermospheric ion composition above Wallops Island during the March 7, 1970 solar eclipse," Goddard Space Flight Center document X-621-71-105, Mar. 1971, also present at Spring AGU, Washington, D.C. (1971).

15. Smith, L. G., C. A. Accardo, L. H. Weeks and P. J. McKinnon "Measurements in the ionosphere during the solar eclipse of 20 July 1963" Journ. Atmos. Terres. Physics, 27, 803, (1965).

16. Spencer, N. W., L. H. Brace, G. R. Carignan, D. R. Taeusch, H. Niemann, "Electron and molecular nitrogen temperature and density in the thermosphere" J. Geophys. Res., 70, 2665, (1965).

17. Spencer, N. W., G. P. Newton, G. R. Carignan and D. R. Taeusch, "Thermospheric temperatures and density variations with increasing solar activity" Space Res. X, North-Holland Publishing Co., p 389, (1969).

18. Stubbe, P., "The F region during an eclipse — a theoretical study" J. Atmos. Terr. Phys., 32, 1109, (1970).

19. Stubbe, P., and S. Chandra, "The effect of electric fields on the F-region behaviour as compared with neutral winds", Journ. Atmos. Terr. Phys., 32, 1909, (1970).

20. Taylor, H. H., L. H. Brace, H. C. Brinton, C. R. Smith, "Direct measurements of Helium and Hydrogen ion concentrations and total ion density to an altitude of 940 kilometers", J. Geophys. Res., 68, 5339, (1963).

21. Taylor, H. A., H. C; Brinton, C. R. Smith, "Positive ion composition in the magneto-ionosphere obtained from the OGO-A satellite, J. Geophys. Res., 70, 5769, (1965).

22. Volland, H. and H. G. Mayr, "A theory of the diurnal variations of the thermosphere", Ann. Geophys., 26, 907 (1970)

23. Volland, H. and H. G. Mayr, "The response of the thermospheric density to auroral heating during geomagnetic disturbances", Journ. Geophys. Res., 76, 3764, (1971).

Table I

NASA 18.104 Tabulation
1800 UT March 7, 1970

Altitude	Measured Parameters									Obscuration
(km)	$n(N_2)$	T_{N_2}	N_i	T_e	$n(O^+)$	$n(N^+)$	$n(NO^+)$	$n(O_2^+)$	$n(N_2^+)$	percent
110	-	-	-	570	-	-	-	-	-	50.0
120	-	-	1.1×10^5	675	-	-	-	-	-	49.6
130	-	-	1.2	790	3.1×10^3	-	8.0×10^4	4.1×10^4	-	49.3
140	-	-	1.4	900	1.1×10^4	-	9.5	5.4	-	49.0
150	3.05×10^{10}	712	1.8	1025	2.8	-	9.8	5.8	-	48.7
160	1.82	783	2.0	1200	5.9	-	9.6	5.6	1.6×10^3	48.4
170	1.14	852	2.2	1375	1.1×10^5	-	8.5	4.9	1.8	47.9
180	7.44×10^9	914	2.4	1540	1.7	1.4×10^3	7.2	4.0	1.9	47.6
190	5.05	967	3.1	1625	2.6	2.0	5.7	3.1	2.0	47.2
200	3.54	1008	4.2	1670	4.1	3.0	4.4	2.5	2.4	46.9
210	2.53	1041	5.6	1695	5.7	3.5	2.9	1.7	2.6	46.5
220	1.85	1065	7.5	1170	7.4	3.7	1.9	1.2	2.6	46.0
230	1.36	1083	9.2	1700	9.3	4.1	1.3	8.1×10^3	2.5	45.6
240	1.02	1097	1.1×10^6	1690	1.1×10^6	4.7	8.5×10^3	5.8	2.4	45.2
250	7.63×10^8	1107	1.3	1660	1.3	6.0	6.5	4.5	2.4	44.7
260	5.75	1116	1.45	1630	1.5	7.3	4.9	3.6	2.4	44.2
270	4.36	1123	1.65	1600	1.7	9.1	4.0	3.0	2.4	43.7
280	3.31	1130	1.7	1555	1.9	1.1×10^4	3.4	2.6	2.4	43.0

Table II

NASA 18.105 Tabulation
1827 UT, March 7, 1970

Altitude	Measured Parameters									Obscuration
(km)	$n(N_2)$	T_{N_2}	N_i	T_e	$n(O^+)$	$n(N^+)$	$n(NO^+)$	$n(O_2^+)$	$n(N_2^+)$	percent
110	-	-	5.7×10^4	504	-	-	-	-	-	93.2
120	-	-	5.0	590	-	-	-	-	-	92.9
130	-	-	6.8	684	1.1×10^3	-	5.1×10^4	1.5×10^4	-	92.5
140	-	-	6.8	790	4.4	-	5.5	2.2	-	92.1
150	3.09×10^{10}	710	7.78	900	1.0×10^4	-	5.8	2.7	-	91.8
160	1.84	780	9.0	1010	2.0	-	5.9	2.7	-	91.4
170	1.16×10^{10}	844	1.05×10^5	1140	4.0	8.3×10^2	6.1	2.6	-	91.0
180	7.54×10^9	907	1.22	1230	6.8	1.1×10^3	5.4	2.3	-	90.7
190	5.07	966	1.50	1310	1.1×10^5	1.3	4.1	1.8	-	90.3
200	3.53	1016	2.0	1375	1.6	1.5	2.9	1.3	-	89.9
210	2.53	1051	2.8	1425	2.3	1.8	2.0	1.0	-	89.4
220	1.84	1078	3.6	1460	3.4	2.2	1.4	8.0×10^3	-	88.9
230	1.37	1096	4.3	1485	4.8	2.7	1.1	6.2	-	88.5
240	1.02×10^9	1110	5.8	1495	6.4	3.3	7.9×10^3	4.7	-	88.0
250	7.70×10^8	1120	8.0	1490	8.2	3.8	5.6	3.5	-	87.5
260	5.83	1128	9.7	1475	9.9	4.5	4.3	2.7	-	86.9
270	4.43	1134	1.15×10^6	1440	1.2×10^6	5.4	3.4	2.1	-	86.3
280	3.38	1139	1.27	1405	1.3	6.4	3.0	1.7	-	85.5

Table III

Jacchia Model, $T_\infty = 1120^\circ K$

Alt.	n(O)	$n(N_2)$	$n(O_2)$	Tg
130	3.5×10^{10}	1.0×10^{11}	1.8×10^{10}	550
140	2.1	5.0×10^{10}	7.6×10^{9}	675
150	1.4	2.8	4.1	785
160	1.03	1.7	2.4	865
170	8.0×10^{9}	1.1	1.5	925
180	6.2	7.8×10^{9}	1.0	975
190	4.9	5.5	6.7×10^{8}	1015
200	4.0	3.9	4.6	1040
210	3.4	2.9	3.4	1060
220	3.7	2.1	2.6	1075
230	2.6	1.5	1.6	1090
240	1.9	1.2	1.2	1100
250	1.6	9.0×10^{8}	8.4×10^{7}	1110

Table IV

a_p, 3-Hour Magnetic Index

DATE \ UT	0-3	3-6	6-9	9-12	12-15	15-18	18-21	21-24
March 6	27	15	15	22	7	18	27	67
7	56	32	15	27	32	39	67	67
8	32	48	67	48	154	207	400	236